

WATER-INDUCED EFFECTS ON THE ADSORPTION ON POLYCRYSTALLINE PLATINUM (II. INTERACTION OF CARBON MONOXIDE AND WATER)

Youn Seok Park, Wha Young Lee* and Ho-In Lee**

Department of Chemical Technology, College of Engineering,
Seoul National University, Seoul 151, Korea

*Department of Chemical Engineering, College of Engineering,
Seoul National University, Seoul 151, Korea

(Received 16 October 1984 • accepted 29 December 1984)

Abstract — The adsorption and desorption of carbon monoxide and water as well as interaction between them on polycrystalline platinum has been studied using the technique of thermal desorption spectroscopy (TDS) under ultrahigh vacuum (UHV) conditions. A small amount of water adsorbs on the surface of the platinum at 310K and desorbs readily and steadily in the temperature range of 350-450 K. When exposure of water by more than 100 L is followed by saturation exposure of carbon monoxide, the height of carbon monoxide desorption peak appeared at 790 K becomes higher. It suggests that preadsorbed water dissociates a small part of carbon monoxide to atomic carbon and oxygen on the surface of the sample. And, interaction of water and carbon monoxide (or atomic carbon) results in the water-gas shift reaction.

INTRODUCTION

Recently, problems on environmental pollution are becoming more serious for the development of industry and the increase in number of automobiles [1]. Problems of emission control from automobile exhaust enforce the research on catalyst which will show the great activity and selectivity for CO oxidation and NO_x reduction [2]. CO is one of the most frequently studied reactants for modern heterogeneous surface science and catalysis because of its relatively simple molecular structure and its simple chemisorptive behavior. H₂O is one of the primary residual gases in UHV system and influences on the many catalytic reactions [3].

The chemisorption of CO on Pt has been studied extensively using LEED [4], work function [5], infrared [6], XPS [7], TDS [8] etc. techniques. CO adsorbs associatively or dissociatively depending on the substrate surface condition and/or the adsorption condition. For example, CO dissociates easily on W and Mo surfaces at even room temperature, not on Pt, Ir and Pd surfaces, and slightly on Ni, Co and Ru surfaces at elevated temperatures [9]. On the other hand, it is reported that Pt can dissociate CO under particular temperature, pressure and surface structure [10]. It is generally accepted for CO/Pt system that (1) adsorption is nondissociative at temperatures less than 600 K, except perhaps at steps

and kinks, (2) techniques involving electron beams must be used cautiously because of a tendency to dissociate CO and leave carbon deposit, (3) the heat of adsorption at low coverage is around 30 kcal mole⁻¹, and (4) the initial sticking coefficient at room temperature is bigger than 0.5 [11].

H₂O adsorbs molecularly on the clean surface of Pt, and H₂O chemisorption has been studied using the techniques of UPS [12], XPS [13], EELS [14] etc. According to TDS results carried out by Fisher and Gland [12], at very low coverages H₂O desorbs at about 180 K, but at coverages higher than 0.05 monolayer a shoulder develops at a temperature less than 170 K, which then shifts to higher temperature with increasing coverage. The TDS spectra of H₂O shows first order at very low coverage but zero order as the coverage increases. Assuming zero order desorption kinetics for the monolayer peak, an activation energy for desorption of about 17 kcal mole⁻¹ is obtained. This value is higher than the sublimation energy of H₂O, 12 kcal mole⁻¹, and so indicates that H₂O is not simply physisorbed on the surface of Pt. The OH group was produced on oxygen-covered Pt and identified [13]. The stoichiometry of the OH group formation between O(a) and H₂O(g) was suggested by Creighton and White [15]. Peng and Dawson reported that preadsorbed water prevented adsorption of hydrogen only at temperatures

** To whom correspondence should be directed.

less than 150 K, the temperature above which water desorbs [16]. Presumably this implies a simple site-blocking mechanism. They also found that oxygen preadsorption stabilized some oxygen-hydrogen containing surface complex till about 300 K.

In this paper we report results for CO and H₂O chemisorptions, H₂O effects on CO chemisorption, and interaction between CO and H₂O on the surface.

EXPERIMENTAL

The experimental apparatus and procedures were almost same as described earlier [17]. A standard ion-pumped vacuum system operating at base pressures about 1×10^{-8} Torr was used. Partial pressures were measured with a quadrupole mass spectrometer, taking into account the fragmentation patterns and sensitivities for various different species. Total pressures were determined using a Bayard-Alpert type ionization gauge and literature values for relative sensitivities of gas components [18].

A polycrystalline platinum foil used in the study was supplied by Materials Research Corporation. The substrate was 0.9 cm x 0.5 cm x 0.0025 cm in size and its nominal purity was 99.99% or higher. The sample was spot-welded to 0.025 cm diameter Ta wire connected to feedthrus which served as current leads for resistive heating. Temperature of the sample was measured with a chromel-alumel thermocouple with a diameter of 0.0127 cm, which was spot-welded on the back side of the sample.

The reagents in this study were CO, H₂, O₂ and H₂O. Except water all the reagents were purchased from Japan Oxygen Company, and their quoted purities were 99.9% (CO), 99.99999% (H₂), and 99.99% (O₂). Except liquid nitrogen trapping, no more purification was given. The H₂O was purified by freeze-thaw distilling and pumping off the nitrogen and oxygen. The purity of the H₂O vapor is unknown, but Fig. 1 shows no O₂ or N₂ peak in a typical mass spectrum after backfilling of H₂O to 1.0×10^{-7} Torr.

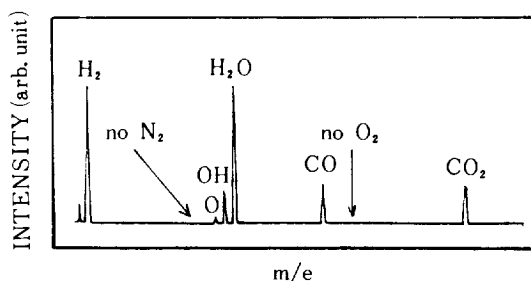


Fig. 1. A typical mass spectrum after backfilling of H₂O to 1.0×10^{-7} Torr.

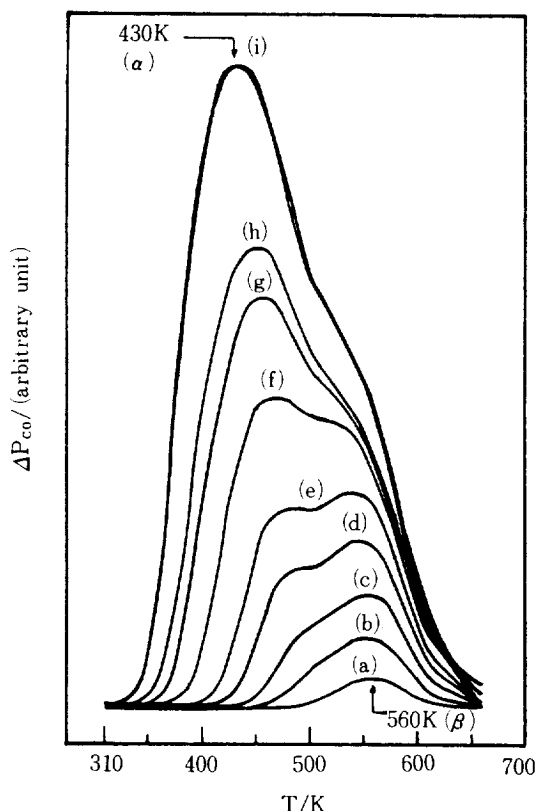


Fig. 2. Carbon monoxide desorption spectra following exposures of the sample to (a) 0.1 L, (b) 1 L, (c) 2 L, (d) 4 L, (e) 6 L, (f) 10 L, (g) 15 L, (h) 20 L, and (i) 50 L and 100 L.

RESULTS AND DISCUSSION

CO TDS spectra

Figure 2 shows CO TDS spectra at various exposures. The adsorption temperature was 310 K and the heating rate was 35 K sec^{-1} . At higher exposures, two desorption states (α state of lower temperature peak and β state of higher temperature peak) exist. As the amount of exposure increases, α state peak position shifts to lower temperature and β state peak position is constant. At saturation the height of α state peak is about 1.5 times higher than that of β state peak. The surface of Pt is saturated by 50 L exposure and α , β saturation peak temperatures are 430, 560 K respectively. CO TDS spectra change sensitively depending on the impurities on the surface. Our thermal desorption results for CO are in good agreement with those of Collins et al. [11]. In desorption orders, α state is suggested to be a first order with an activation energy dependent on coverage and β

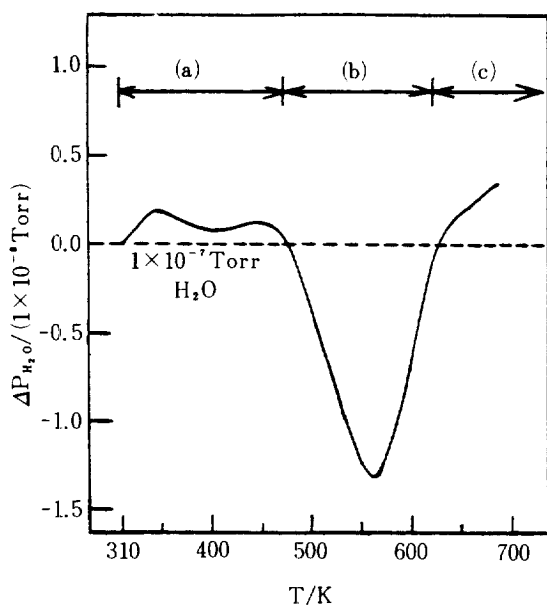


Fig. 3. A typical water spectrum after a 5 L water exposure at 310 K. Region (a), (b), and (c) correspond to the region of (a) desorption, (b) dissociation of water and interaction between H_2O and CO, and (c) side effects.

state a first order with that independent of coverage. The competitive adsorption between these two adsorption states is expected because the heights of both peaks get higher at the same time with increasing the exposure of CO. The TDS spectra obtained by Hopster and Ibach on Pt 6(III)×(III) are very similar to ours [10]. This suggests that some steps exist on the surface of our Pt.

Chemisorption of H_2O

Figure 3 shows a typical water desorption spectrum after 5 L exposure at 310 K. At the beginning of the flash most portion of the background was H_2O at about 1×10^{-7} Torr due to its low pumping speed. This spectrum can be divided into three regions: (a) the region between 310 K and 470 K, (b) the region between 470 K and 610 K, and (c) the region over 610 K.

Region (a) of Fig. 3 is suggested to be the region of H_2O desorption. We attribute this peak to the desorption of water with the following reasons: First, at a constant temperature the area of desorption curve becomes bigger proportional to available adsorption sites as seen in Fig. 4. Second, at a given exposure the amount of adsorbed H_2O depends on adsorption temperature, that is, the peak area increases with lowering adsorption temperature as seen in Fig. 5. The pressure of H_2O is reduc-

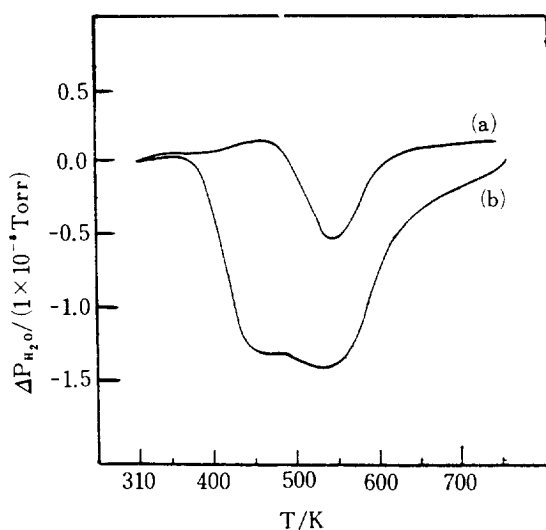


Fig. 4. Water spectra under a constant leak of 1×10^{-7} Torr of H_2O , (a) without and (b) with a predosed 3 L CO at 310 K.

ed at about 400 K during flash. This suggests that a small amount of H_2O readsorbs on the empty adsorption sites produced by desorption of hydrogen. This readsorbed water desorbs easily with continuous elevation of temperature, which results in a small peak near 450 K. However, we could not completely rule out the heterogeneity of the sample surface for the widely outcoming range (350-470 K) of region (a) in Figs. 3 and 5.

Region (b) of Fig. 3 is suggested to be the region in which two processes occur. First, desorption of CO adsorbed from background gives empty adsorption sites and H_2O adsorbs transiently on those sites. Second, the adsorbed CO and gaseous H_2O prepare to give a water-gas shift reaction. We consider a complex $CO(a)-H_2O(g)$ or $C-O(a)-H_2O(g)$ as an intermediate of severe endothermic water-gas shift reaction. This complex produces H_2 and CO_2 with the helps of Pt catalyst and of energy supplied by elevating temperature, where $C-O(a)$ implies the dissociative adsorption of CO. With the above reasons it seems that another peak near 800 K on H_2 TDS curve appears [17].

Region (c) is assigned to side effects such as the desorption from lead-wires by elevating temperature. The extent of the rise from the starting level increases with the final temperature of desorption or with holding time at a fixed final temperature. The above phenomena were also observed on Ru(001) [19].

Figure 4 shows H_2O TDS spectra under a constant leak of 1×10^{-7} Torr of H_2O . Curves (a) and (b) correspond to the spectra from a clean surface and a surface

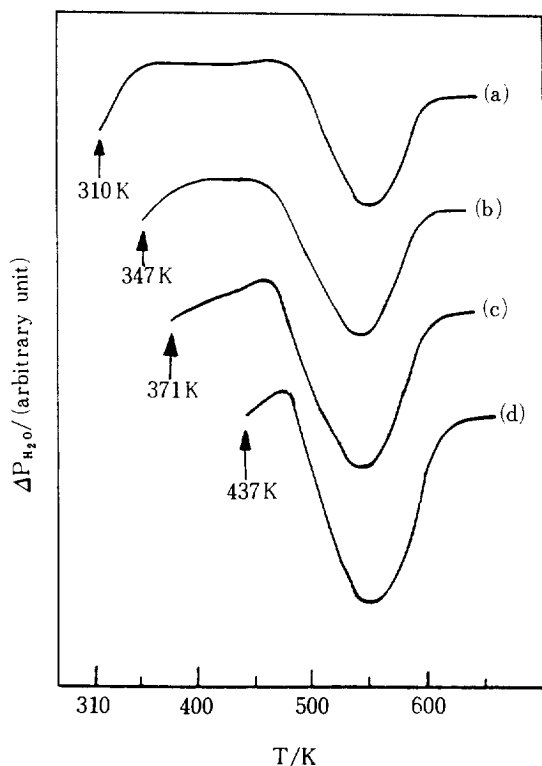


Fig. 5. Water spectrum for four different adsorption temperatures; (a) 310K, (b) 347K, (c) 371K, and (d) 437K.

predosed 3 L CO at 310 K, respectively. Curve (b) gives the result that a large amount of gaseous H_2O is consumed by CO adsorbed on the surface of the sample for water-gas shift reaction and by empty adsorption sites produced by desorbing CO. Unlike curve (a), in curve (b) no desorption peak appears at lower temperatures. This suggests that preadsorbed CO inhibits the adsorption of H_2O .

Figure 5 shows 5 L H_2O TDS spectra adsorbed at (a) 310 K, (b) 347 K, (c) 371 K, and (d) 437 K, respectively. The results show that the area of the convex peak is strongly related to the adsorption temperature, i.e., the higher the adsorption temperature, the smaller the desorption area. When H_2O adsorbs at temperature higher than hydrogen desorption temperature (380-430 K depending on coverage), the reduced part of H_2O pressure shown in region (a) of Fig. 3 was not found. This result gives a backup to our discussion about the region (a) of Fig. 3. The depth of the curve in the region (b) of Fig. 3 becomes deeper with increasing adsorption temperature since CO partial pressure in the system increases with experimental period due to the

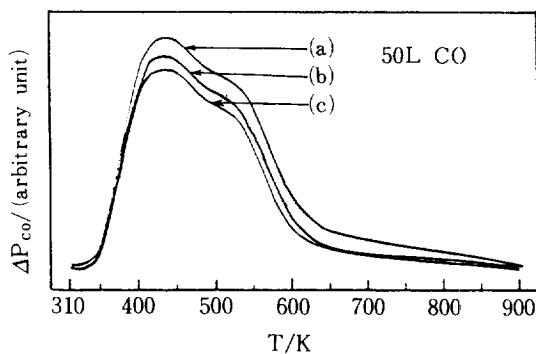


Fig. 6. CO desorption spectra after (a) 50 L CO exposure, (b) 50 L CO exposure followed by 90 L H_2O and flashed under 3×10^{-4} Torr of H_2O , and (c) 50 L CO exposure followed by 180 L H_2O and flashed under 6×10^{-4} Torr of H_2O .

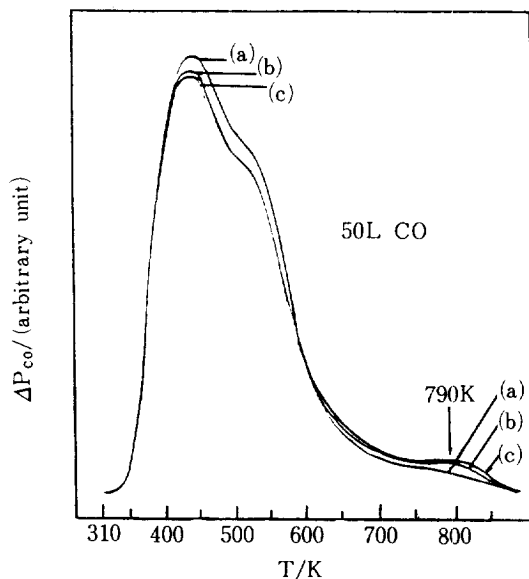


Fig. 7. 50 L CO desorption spectra (a) without, and with (b) pre-dosed 300 L H_2O and (c) pre-dosed 500 L H_2O .

formation of CO by reaction between gaseous H_2O and C on the QMS and BAG filaments.

H_2O effects on the adsorption of CO

Figure 6 shows CO TDS spectra after 50 L CO exposure followed by different H_2O exposures. The area of CO desorption curve decreases with increase in the partial pressure of H_2O . It indicates that adsorbed CO is consumed by gas phase H_2O for water-gas shift reaction.

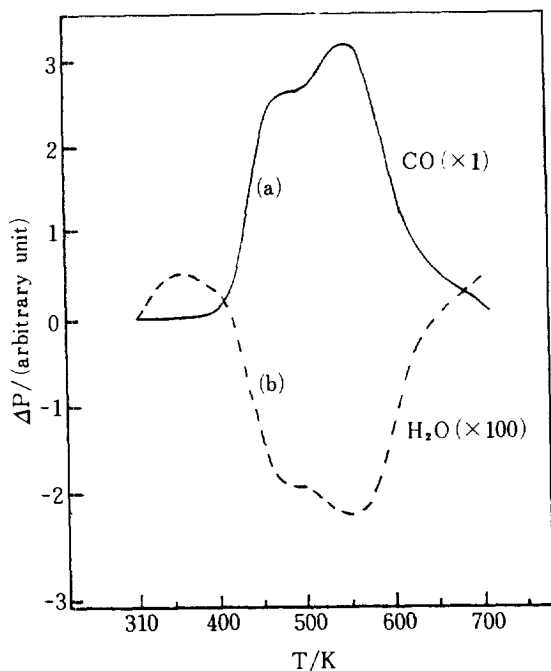


Fig. 8. H₂O and CO spectra from the surface predosed with a 3 L CO and under a constant leak of 1×10^{-7} Torr of H₂O. QMS sensitivity is increased by 100 for water spectrum.

According to the results of another experiment, postdosed H₂O does not effect on the process of CO desorption.

In Fig. 7 curves (a), (b), and (c) show 50 L CO desorption spectra without predosing H₂O, with predosing 300 L H₂O, and with predosing 500 L H₂O, respectively. The experimental result about reverse exposure sequences (in Figs. 6 and 7) shows the limit of adsorption ability of H₂O at temperatures above 310 K. We observe an interesting fact that with increasing predosed H₂O the height of CO desorption peak near 800 K becomes higher. This peak position is at about 790 K. It seems that this peak is caused from dissociative adsorption of CO. From the above facts we suggest as follows: (1) Predesorbed H₂O dissociates CO into C(a) and O(a). (2) At near 790 K some surface carbon atoms combine with surface oxygen atoms to give CO and some others react with gaseous H₂O producing CO and H₂O [$C(a) + H_2O(g) \rightleftharpoons CO(g) + H_2(g)$]. We could not obtain CO₂ desorption peak near 790 K in QMS experiments and this explains indirectly that near 790 K water-gas shift reaction occurs via C(a), but not CO(a). In Fig. 6, it is suggested that postdosed H₂O does not change the height of CO desorption peak near 790 K

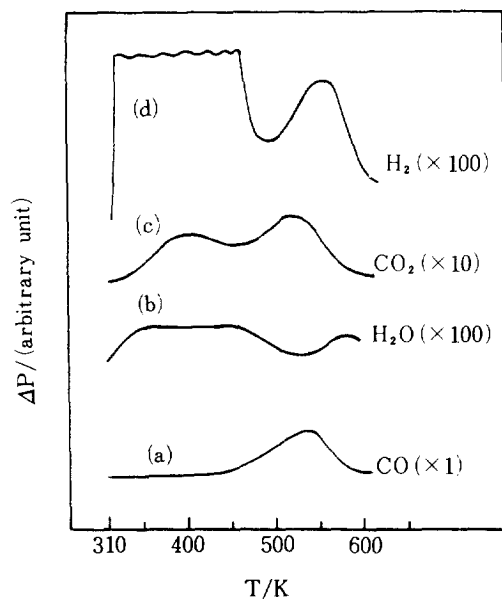


Fig. 9. Various desorption spectra derived from 2.0×10^{-8} Torr background pressure exposure for 2 min. QMS sensitivities of each spectrum are shown in parentheses.

because the amount of adsorbed H₂O given by postdosing H₂O is too small.

Interaction between CO and H₂O

Figure 8 shows a CO [curve (a)] and an H₂O [curve (b)] spectra from the surface predosed 3 L CO and under a constant leak of 1×10^{-7} Torr H₂O. CO and H₂O spectra are in the relation of mirror image except H₂O desorption peak at about 350 K. This suggests that the concave peak is due to the combined phenomenon of the dissociation of water and the reaction between H₂O and CO.

Figure 9 shows CO, H₂O, CO₂ and H₂ spectra derived from adsorbing at 2.0×10^{-8} Torr background pressure for 2 min. Comparing the peak temperature of each spectrum one another, we believe that CO interacts with H₂O producing H₂ and CO₂. It is considered that the peak position of H₂ shifts toward higher by 50 K than that of CO because the desorption of hydrogen formed by water-gas shift reaction is delayed by CO as suggested by Nishiyama and Wise that there is some time-lag by forming a transient intermediate complex (H-CO) during the displacement of chemisorbed monoxide[20].

CONCLUSION

- (1) A small amount of water adsorbs on the surface of

the platinum at 310 K and desorbs readily and steadily in the temperature range of 350-450 K.

- (2) Water preadsorbed by more than 100 L at 310 K dissociates a small part of carbon monoxide to atomic carbon and oxygen on the surface of the sample.
- (3) Interaction between gaseous water and carbon monoxide (or atomic carbon) on the surface results in the water-gas shift reaction which shows its maximum rate at about 790 K.
- (4) A small amount of water readsorbs transiently on the empty adsorption sites produced when hydrogen desorbs near 400 K.

Acknowledgements

This research was supported in part by the Ministry of Education and by Yukong Limited.

NOMENCLATURE

C(a), CO(a), O(a): adsorbed species considered
 C-O(a): dissociatively adsorbed CO
 CO(g), H₂(g), H₂O(g): gas-phase species considered
 EELS: electron energy loss spectroscopy
 K: kelvin(s) as a unit of absolute temperature
 L: langmuir(s) as a unit of exposure
 LEED: low-energy electron diffraction
 Pt 6(111)x(111): Miller index of a stepped platinum surface
 QMS: quadrupole mass spectroscopy
 Ru(001): Miller index of the basal plane of ruthenium
 TDS: thermal desorption spectroscopy
 UHV: ultra-high vacuum
 UPS: ultra-violet photoelectron spectroscopy
 XPS: X-ray photoelectron spectroscopy

REFERENCES

1. Perkins, H.C.: "Air Pollution", McGraw-Hill, Tokyo, 1974.
2. Gorte, R.J. and Schmidt, L.D.: *Surface Sci.*, **111**, 260 (1981).
3. Lee, H. -I., Koel, B.E., Daniel, W.M. and White, J.M.: *J. Catal.*, **74**, 192 (1982).
4. Ertl, G., Neumann, M. and Streit, K.M.: *Surface Sci.*, **64**, 393 (1977).
5. Morgan, A.E. and Somorjai, G.A.: *Surface Sci.*, **12**, 405 (1968).
6. Shigeish, R.A. and King, D.A.: *Surface Sci.*, **58**, 379 (1976).
7. Bonzel, H.P. and Fisher, T.E.: *Surface Sci.*, **51**, 213 (1975).
8. McCabe, R.W. and Schmidt, L.D.: *Surface Sci.*, **66**, 101 (1977).
9. Nieuwenhuys, B.E.: *Surface Sci.*, **126**, 307 (1983).
10. Hopster, H. and Ibach, H.: *Surface Sci.*, **77**, 109 (1978).
11. Collins, D.M., Lee, J.B. and Spicer, W.E.: *Surface Sci.*, **55**, 389 (1976).
12. Fisher, G.B. and Gland, J.L.: *Surface Sci.*, **94**, 446 (1980).
13. Fisher, G.B. and Sexton, B.A.: *Phys. Rev. Lett.*, **44**, 683 (1980).
14. Ibach, H. and Lehwald, S.: *Surface Sci.*, **91**, 187 (1980).
15. Creighton, J.R. and White, J.M.: *Surface Sci.*, **122**, L648 (1982).
16. Peng, Y.K. and Dawson, P.T.: *Can. J. Chem.*, **55**, 1658 (1977).
17. Park, Y.S. and Lee, H. -I.: *J. Korean Inst. Chem. Engrs.*, **23**(1985), accepted.
18. Summers, R.L.: NASA Technical Note TND-5285, National Aeronautics and Space Administration, Washington, D.C., June 1969.
19. Lee, H. -I. and Lee, M. -D.: *J. Korean Inst. Chem. Engrs.*, **20**, 355 (1982).
20. Nishiyama, Y. and Wise, H.: *J. Catal.*, **32**, 50 (1974).